Journal of the Korean Physical Society, Vol. 55, No. 2, August 2009, pp. 681∼687

Validation of a GATE Model for the Simulation of a Trionix TRIAD SPECT Camera

Min-Jae Park and Kwang-Suk Park*
Interdisciplinary Program, Biomedical Engineering Major, Seoul National University, Seoul 110-744

Jae-Sung Lee, Yu-Kyeong Kim and Dong-Soo Lee
Department of Nuclear Medicine, Seoul National University College of Medicine, Seoul 110-744

(Received 3 February 2009, in final form 16 April 2009)

The aim of this study was to validate a GATE simulation for the Trionix TRIAD triple head SPECT camera. Experimental and simulated physical characteristics, such as the energy spectrum and resolution, the system sensitivity, and the spatial resolution, were compared. The energy spectrum of the TRIAD was analyzed by using averaged screen-captures of the screen out MCA window and a linear interpolation of the graph. The energy resolution of 140 keV gamma rays was measured without the collimator. To measure the system sensitivity, we measured counts from a Tc-99m point source five times and averaged the results. The spatial resolution was measured from the profile of the line source aligned along the x-axis by using the bi-linear interpolation method. The tests were performed at various distances with a LEUHR parallel-hole collimator for further research on brain scans. The energy window was set to 126 $\sim$ 154 keV for the simulation and to 140 keV $\pm$ 20% for the real detector. The shapes of the normalized energy spectra were identical. The energy resolution was 10.1% in the experiment and 9.9% in the simulation, for a 10.1% resolution setting. The sensitivities at various distances (5 cm, 10 cm, 15 cm, and 20 cm) were almost identical. Simulation results (66 counts/sec/MBq) were higher than real experiment results (63 counts/sec/MBq). The spatial resolutions of the simulation data (4.7, 6.3, 7.9, and 9.7 mm) were also comparable to those of real experiments (4.4, 5.8, 7.5, and 9.1 mm). Overall the comparisons showed good agreements between the experimental and the simulation studies. The error levels were roughly 5%, what would be small enough to use the GATE simulation for further MonteCarlo-simulation-based investigations.

PACS numbers: 87.57.Ce
Keywords: Monte Carlo simulation, Validation, Analysis method, SPECT

I. INTRODUCTION

The Monte Carlo (MC) simulation is widely used in the field of nuclear medicine because it overcomes all limitations; typically, limitations are on radioisotopes and cameras. The production of radio sources is limited to a facility that houses a cyclotron or nuclear reactor. Only a high-power cyclotron and a reactor can produce radioisotopes that emit high-energy gamma rays. Radio sources produced at one facility can be transferred to other facilities; however, natural decay imposes temporal limitations on the transfer. Further, it is not possible to change the detector module of commercial cameras. A new scintillation crystal and algorithm for a digitizer can be determined by using a simulation, *i.e.*, without requiring the use of any facilities. Furthermore, novel image processing algorithms can be developed by simulations that provide rich information.

Geant4 Application for Emission Tomography (GATE) is a general MC simulation package that is capable of simulating gamma cameras such as PET and SPECT [1, 2]. However, because simulations are not real, validations between GATE and real cameras are essential; such validations have been carried out for several commercial cameras [3–9]. For example, Axis (Philips Medical) and DST Xli (GE Healthcare) SPECT cameras have been validated in terms of their energy spectra, energy resolution, sensitivity, and spatial resolution, with 5% differences. The difference in spatial resolutions obtained using a water phantom was as high as 12% [6,9]. On the basis of these validations, results of other processing methods are predictable within acceptable error limits.

*E-mail: kspark@bmsil.snu.ac.kr; Fax: +82-2-745-7870

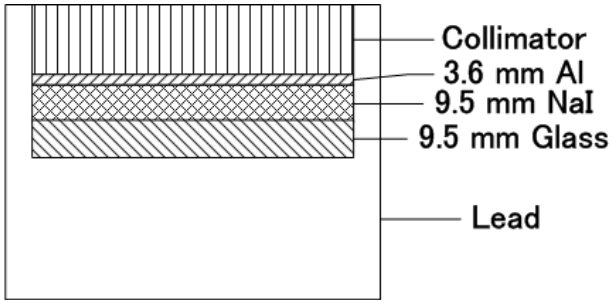

Fig. 1. Schematic of the Trionix TRIAD XLT9 triple-head SPECT detector.

Table 1. Specifications of the Trionix TRIAD XLT9 triple-head SPECT detector.

Description	Type or Dimension
Field of view	20.0 cm × 40.0 cm
Crystal material	NaI (Tl)
Crystal thickness	9.5 mm (3/8")
Photomultiplier tubes	49

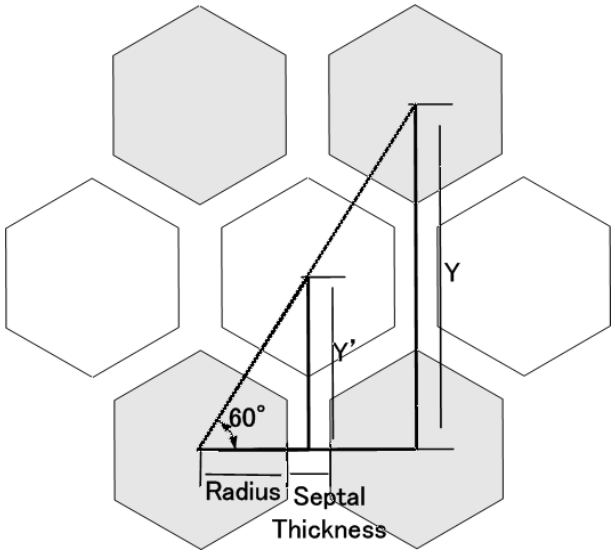

Fig. 2. Schematic of the hole pattern on the collimator. Two kinds of hole patterns were interwovea in order, and holes were formed at distances calculated using the similarity of triangles.

The main objective of this study was to validate the MC simulation of the Trionix Triad SPECT camera. In addition, performances of various analysis methods were evaluated.

II. EXPERIMENTS

1. Simulation Setup

GATE consists of the CLHEP library and Geant4 package, which have been widely used in high energy physics [2]. Equipped with such reliable libraries, GATE is a high-level front-end framework that can use script-based commands; further, it can simulate time-dependent movement and dose calculations. However, since GATE simulates every photon track and lacks any techniques for variance reduction, GATE simulations require a longer time than dedicated simulation packages [10].

GATE version 3.12 was run on a quad core Linux machine (Ubuntu 6.06). To reduce the total simulation time, it is split into multiple simultaneous processes with different time periods by the program "job splitter" [11]. Result files of the split simulations were merged using a "file merger". Even though a clustered simulation was performed, each simulation required almost one week. The result files were exported to MATLAB 7.8 (MathWorks, MA, USA) by ROOT 5.20 (Cern, Switzerland); the files were in the ASCII format and contained essential information such as source number, energy, and detected position.

Triad XLT9, simulated in this study, is a triple-head SPECT camera manufactured by Trionix Corporation, OH, USA. Each detector of this camera consists of a 0.95 cm-thick 40 × 22 cm^2 NaI(Tl) crystal, a 0.95 cm-thick back-scattering glass, and a 0.36 cm-thick aluminum front cover [Fig. 1, Table 1]. A total of 49 photomultiplier tubes (PMTs) are used to read out events. The extent of interaction of the camera with other components is small and, therefore, is assumed to be negligible [9].

$$X = 2 \times R + T$$
$$Y = X \times \tan\left(\frac{\pi}{3}\right), \quad (1)$$

where X, Y, R, and T are the distances between two adjacent air-holes on the x and the y axis, the radius, and septal thickness, respectively. The doubled distances of the white-colored air-hole pattern are calculated as follows:

$$X' = \left(\frac{X}{2}\right)$$
$$Y' = X' \times \tan\left(\frac{\pi}{3}\right), \quad (2)$$

where X' and Y' are the distances between white and gray colored hole-patterns on the x and the y axis, respectively.

A low-energy ultra-high-resolution (LEUHR) collimator used for a brain scan was selected. A box-shaped collimator made of lead was simulated in GATE. To cover the collimator with hexagonal air holes in GATE, a hexagonal air-hole pattern was doubled, with a pitch of 1.5 between the hexagonal holes, as the white and the gray color shown in Fig. 2. The repetition distance

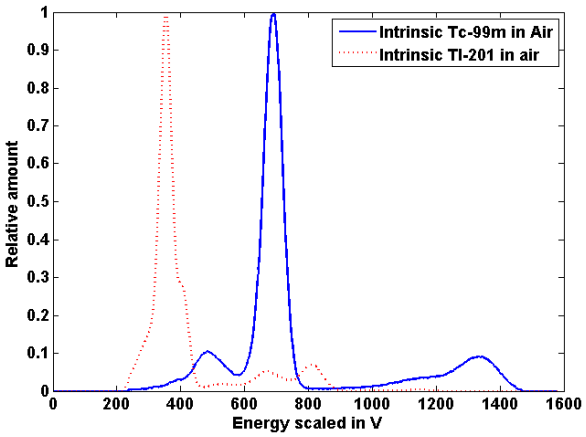

Fig. 3. Intrinsic resolutions from point sources of Tc-99m and Tl-201 without an additional phantom. The scale of the x-axis is not keV. Real energy should be restored by an interpolation of the known sources.

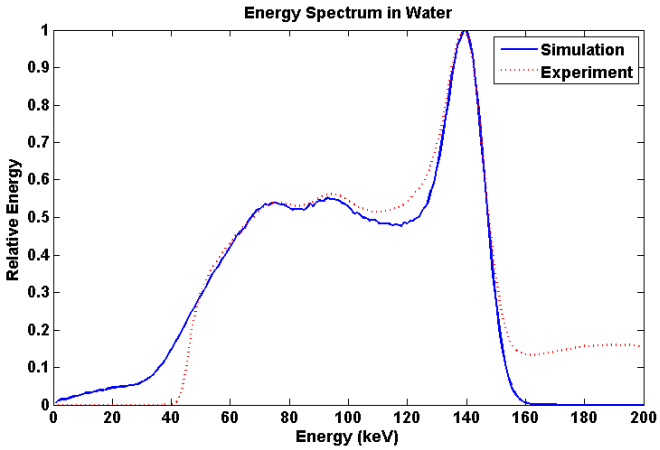

Fig. 4. Energy spectrum of a Tc-99m point source placed in a water phantom. The blue solid and the red dotted lines show the simulated and the experimental energy spectra, respectively.

was calculated from the radius and the septal thickness listed on the specification sheet. Distances between the gray-colored air-holes were calculated as follows:

2. Comparison of Physical Characteristics

A. Energy resolution

Energy spectra were obtained from screen-captured spectral images of bundled software, multi-channel analyzer (MCA). For the normalization of event counts, measured energy spectrum on the MCA window were scaled to have the same area under the curve. Because the energy axis of the MCA program was not scaled in keV, real energy had to be restored by an interpolation between peaks of known energy [Fig. 3]. Steps for estimating the energy spectra were as follows: First, the size of the MCA window was increased as much as possible in order to achieve the maximum expansion of the energy axis (x-axis). Second, 10 images, each with an acquisition time of 10 s, were averaged to eliminate small fluctuations. The total time required for averaging the energy spectrum was 100 s. Third, the photopeak energies of Tc-99m and Tl-201 were assumed to be 140.5 keV and 70.8 keV, respectively. Fourth, positions of energies of 0 and 200 keV on the energy axis were determined by linear extrapolation with a 1 keV/pixel scale. Then, to calculate the energy resolution, we calculated the full width at half maximum (FWHM) of the photopeak by using two methods. In the first method, the distance of over the half maximum count of the photopeak window was determined according to the NEMA (National Electrical Manufacturers Association) NU 1−2001 (hereafter referred to as the NEMA method) [12]. In the second method, the standard deviation of the Gaussian fitting over half the maximum count of the photopeak window was calculated (hereafter referred to as the Gaussian fitting method) [13]. The Gaussian fitting was carried out by using the nonlinear least squares method with a trust region algorithm. The FWHM was calculated as follows:

$$FWHM = 2\sqrt{2\log(2)} \times \sigma \tag{3}$$

where σ is standard deviation of fitted Gaussian.

In the GATE simulation, Gaussian blurring is used to realize the energy distribution. Because the energy resolution calculated from the simulation data was slightly different from the corresponding resolution set in the GATE simulation code, the input energy blurring value was optimized to the value obtained from the actual detector. A total of 4000 million events were generated.

B. System Sensitivity

A Tc-99m point source with an activity of 5.96 MBq (approximately 1 ∼ 2 ml), placed in air, was measured using a collimator. The distances of this point source from the detector were 5, 10, and 20 cm. Further, a Tc-99m point source with an activity of 14.43 MBq was placed at the center of the Jaszczak SPECT Phantom (Biodex Medical System, NY, USA) filled with water without any inside structure. Distances of this point source from the detector were center, 5.5 cm, and 8.5 cm [Fig. 5]. The distance between the detector and the phantom surface was fixed at 10 cm. Counts measured in 300 sec were corrected for radiation decay. A 20% symmetrical energy window was applied. As mentioned previously, a total of 4000 million events were generated in the GATE simulation. The probability of the point sources emitting a gamma ray per disintegration was 89% [14]. The estimated sensitivities were represented in unit of counts/sec/MBq.

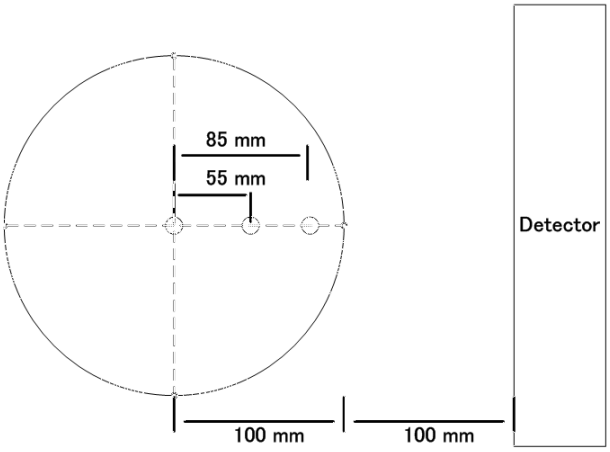

Fig. 5. Schematic of measurements for the sensitivity. A point source was placed at the center, 5.5 cm and 8.5 cm to the detector.

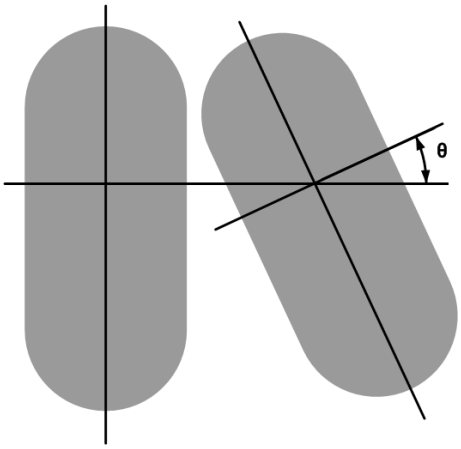

Fig. 6. Effect of rotation on the calculation of the spatial resolution. A line profile rotated by an angle is miscalculated by a factor of $1/\cos(\theta)$.

C. System Spatial Resolution

A Tc-99m line source with a 19 MBq activity and a 1.2-mm-inner diameter was measured with a collimator in air. The distances of this line source from the detector were 5, 10, 15, and 20 cm. A 20% symmetrical energy window was applied. The pixel pitch of the projection image was 0.445 mm, and the pixel size was 512 × 1024. Since line profiles on the image were not parallel to an axis, an image rotated by an angle was miscalculated by a factor of $1/\cos(\theta)$ [Fig. 6]. Therefore, the image was re-aligned at an angle-θ by bilinear interpolation. In this case as well, a total of 4000 million events were generated in the GATE simulation. FWHM values calculated by using the NEMA method and Gaussian fitting method were compared. Because of ill-conditioned events on the axial distribution, some Gaussian fittings were unsuccessful and excluded. The FWHM of the summed line profile and averaged FWHMs of each line profile were also compared. In order to determine the effect of pixel size, we set the pixel pitches of the projection image to 0.445, 0.89, and 1.78 mm. NEMA recommends that the average FWHM of each line profile, which is measured at a distance of 10 cm away from the collimator surface, and that the pixel size should be one-tenth the spatial resolution.

III. RESULTS

1. Energy Spectrum

The energy spectrum of the MC simulation was identical to that estimated experimentally. The shapes of the energy spectra in the photopeak window were identical. However, there were no events below 40 keV and no scatter event above 160 keV [Fig. 4]. No events were observed below 40 keV because the electronics of TRIAD are assumed to have cut events of very low energy. Events above 160 keV was assumed to be scatter events due to contamination of a high energy source, such as Mo-99 [15]. There was good agreement between the screen-captured spectrum and the spectrum obtained by the MC simulation; therefore, the screen capture method was effective in estimating the spectral distribution. The exact energy was determined by a linear interpolation and an extrapolation of the two photopeak energies from the Tc-99m and Tl-201 sources [Fig. 3]. Energy resolutions calculated by using the NEMA and the Gaussian fitting methods were 10.7% and 10.1%, respectively, while the energy resolution listed on the specification sheet was 9.6% to 9.8% (UFOV, typical to worst case). Using the Gaussian fitting method, energy resolutions calculated in the GATE simulation were 9.55% 10.38% while the corresponding input values for energy blurring were 9.4% $\sim$ 10.2%, respectively [Table 2]. Further, FWHMs calculated by using the NEMA method

Table 2. Energy resolution (at a photopeak energy of 140 keV) calculated by using a simulation with different setting values for the energy blurring. The NEMA method yields insensitive results in images with wide energy bins. The energy resolutions are expressed in units of %.

Blurring	NEMA	Gaussian Fitting
9.4	9.25 ± 0.00	9.55 ± 0.02
9.5	9.82 ± 0.32	9.68 ± 0.02
9.6	9.96 ± 0.00	9.77 ± 0.01
9.7	9.96 ± 0.00	9.88 ± 0.01
9.8	9.96 ± 0.00	9.99 ± 0.01
9.9	9.96 ± 0.00	10.07 ± 0.02
10.0	9.96 ± 0.00	10.19 ± 0.01
10.1	10.68 ± 0.00	10.28 ± 0.02
10.2	10.68 ± 0.00	10.38 ± 0.02

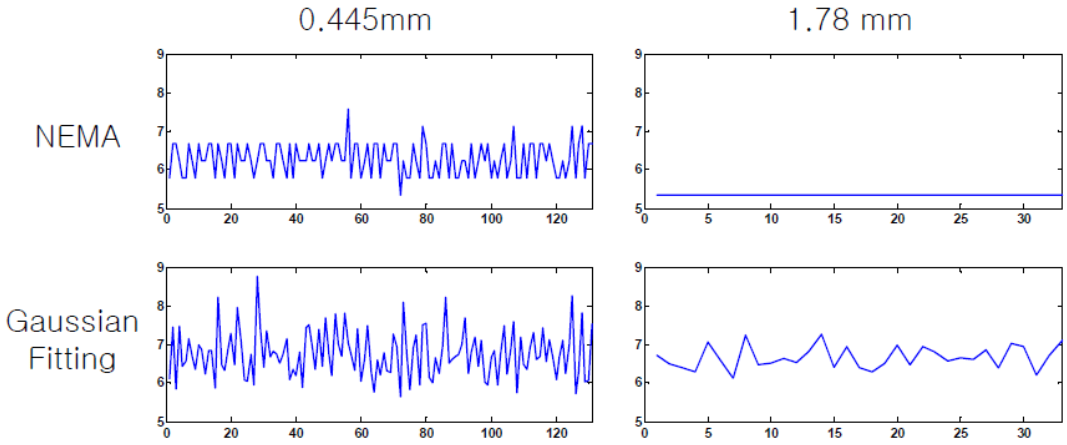

Fig. 7. Spatial resolutions at 10 cm calculated by using the NEMA (upper rows) and the Gaussian Fitting (lower rows) methods with two pixel sizes, 0.445 mm (left columns) and 1.78 mm (right columns).

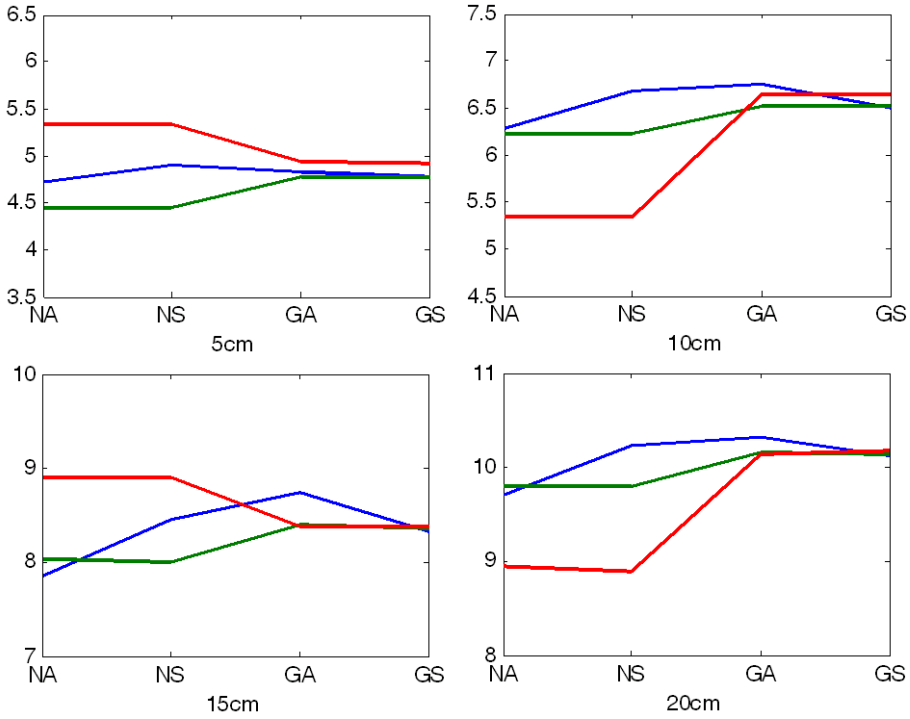

Fig. 8. Spatial resolutions of various pixel sizes and calculation methods. Blue, green, and red lines represent pixel sizes of 0.445, 0.89, and 1.78 mm, respectively. NA, NS, GA, and GS are the averaged FWHMs of each profile and the FWHM of the summed profile, which are calculated by using the NEMA method and the Gaussian fitting method, respectively.

were fixed to 9.96% while input values for energy blurring changed from 9.5% to 10.0%. In subsequent simulations, the input value for energy blurring was set to 9.9%.

2. System Sensitivity

System sensitivities were almost the same over all distances, mainly because the collimator effectively limits the direction of the photons. The overall sensitivity of the experiment was 63.04 ± 0.51 counts/sec/MBq while that listed on the specification sheet was 67.6 counts/sec/MBq [Table 3]. The sensitivity of the simulation was 65.52 ± 0.78 counts/sec/MBq. Depth-dependent sensitivities of the water phantom at depths of 2.5, 5.5, and 11 cm were 53.38 ± 0.10, 39.90 ± 0.24, and 22.31 ± 0.26 counts/sec/MBq in the experiment and 52.27 ± 0.22, 38.46 ± 0.23, and 20.22 ± 0.19 counts/sec/MBq in the simulation, respectively. The

Table 3. System sensitivities in air at various distances from the collimator surface (upper rows), and sensitivities in a water phantom at various depths from the water phantom surface (lower rows). The distance between the water phantom surface and the collimator surface was 10 cm. Sensitivities are expressed the units of counts/sec/MBq.

	Simulation	Experiment
5 cm	66.10 ± 0.63	63.26 ± 0.63
10 cm	65.53 ± 0.43	62.56 ± 0.25
20 cm	65.12 ± 0.48	63.28 ± 0.22
2.5 cm	52.27 ± 0.22	53.38 ± 0.10
5.5 cm	38.46 ± 0.23	39.90 ± 0.24
11 cm	20.22 ± 0.19	22.31 ± 0.26

Table 4. Spatial resolution calculated from experiment. The averaged FWHM of each profile and the FWHM of the summed profile, which are calculated by using the NEMA method and the Gaussian fitting method, are compared. FWHMs are expressed in units of mm.

	NEMA		Gaussian Fitting	
Distance	Average	Sum	Average	Sum
5 cm	4.44 ± 0.29	4.45	4.48 ± 0.25	4.49
10 cm	5.83 ± 0.34	5.79	5.97 ± 0.33	5.98
15 cm	7.45 ± 0.41	7.57	7.59 ± 0.41	7.69
20 cm	9.12 ± 0.47	9.35	9.40 ± 0.40	9.47

overall difference in sensitivities was approximately 2 counts/sec/MBq.

3. Spatial Resolution

The spatial resolution calculated by using the simulation was almost identical to that calculated from the experiment. As recommended by NEMA, the spatial resolutions calculated from the experiment were 4.44, 5.83, 7.45, and 9.12 mm while those calculated by using the simulation were 4.72, 6.29, 7.86, and 9.69 mm [Table 4, Fig. 8]. The overall difference in resolution was approximately 0.4 mm. These results were acceptable because the collimator resolution listed on the specification sheet was 6.15 mm at a distance of 10 cm from the collimator. Various methods for calculating spatial resolution were tested. The rotated profile caused degradation in the spatial resolution calculated from the data of the actual camera. However, the angles of the rotated profile on the projection image were less than 0.5°, and the amount of degradation was 0.02%. FWHMs calculated from the realigned profile were almost the same as those calculated from the original profile; this similarity can be attributed to the small angles. However, the differences in spatial resolutions calculated by using the NEMA method were greater than those calculated experimentally and by using the Gaussian fitting method. For the summed profile, the discrimination ability of the NEMA method was low. With regard to pixel size, images with different pixel sizes were generated using a simulated projection data [Table 5]. The NEMA method yielded less sensitive results in the case of low-resolution images, *i.e.*, large pixel sizes. In contrast, the Gaussian fitting method was robust to variations in pixel size and sensitive to fluctuations in event count [Fig. 5]. Overall, the spatial resolutions calculated by using the Gaussian fitting method were greater than those calculated by using the NEMA method. The error levels were roughly 5% overall.

Table 5. Spatial resolution calculated from the simulation. The averaged FWHM of each profile and the FWHM of the summed profile, which are calculated by using the NEMA method and the Gaussian fitting method, are compared. FWHMs are expressed in units of mm.

		NEMA		Gaussian Fitting	
Distance	Pixel-Size	Average	Sum	Average	Sum
5 cm	0.445 mm	4.72 ± 0.30	4.90	4.83 ± 0.35	4.78
	0.89 mm	4.45 ± 0.00	4.45	4.77 ± 0.19	4.77
	1.78 mm	5.34 ± 0.00	5.34	4.93± 0.11	4.92
10 cm	0.445 mm	6.29 ± 0.42	6.68	6.76 ± 0.62	6.49
	0.89 mm	6.23 ± 0.00	6.23	6.53 ± 0.23	6.52
	1.78 mm	5.34 ± 0.00	5.34	6.66 ± 0.30	6.65
15 cm	0.445 mm	7.86 ± 0.55	8.46	8.76 ± 0.96	8.32
	0.89 mm	8.04 ± 0.15	8.01	8.40 ± 0.37	8.36
	1.78 mm	8.90 ± 0.00	8.90	8.38 ± 0.23	8.39
20 cm	0.445 mm	9.69 ± 0.62	10.24	10.33 ± 0.72	10.13
	0.89 mm	0.78 ± 0.11	9.79	10.15 ± 0.31	10.14
	1.78 mm	0.95 ± 0.31	8.90	10.15 ± 0.26	10.18

IV. CONCLUSION

All simulations were performed on the basis of the specification sheet provided by the manufacturer. GATE simulation results were almost in agreement with the results of actual experiments; however, differences could be caused by a minor physical process not implemented in the GATE simulation, an impurity in the radio-source, such as Mo-99 which is the mother source of Tc-99m, or an implementation method of the MonteCarlo simulation, such as the step size for calculating probabilities not being continuous as in the real world [1,2,10,15].

Sensitivities were slightly different between values calculated from the experimental data, values listed on the specification sheet, and values calculated from the simulation. Mismatches between values listed on the specification and those calculated from experimental data could be caused by the difference in energy windows. The sen-

sitivity on the specification follows the NEMA standard, and NEMA recommends a 15% energy window; however, a 20% energy window was used for the Triad camera because the actual experiments were based on the patient scan. Since a narrower energy window causes a lower sensitivity, lower sensitivities in experiments could be caused by external factors, such as low efficiency of electronics.

The spatial resolutions calculated by using the NEMA method and the Gaussian fitting method were similar; however, these methods used different features for the calculations. In the NEMA method, distance was used for calculation purposes; therefore, unit size would be a major factor limiting discrimination resolution. Tests related to energy resolution showed that the NEMA method could not discriminate small variations in the energy resolutions. Tests related to spatial resolution showed that a large pixel size was the cause of insensitivities in the spatial resolutions calculated by using the NEMA method. As mentioned previously, the Gaussian fitting method was found to be robust to variations in pixel size and sensitive to fluctuations in event count. Therefore, the application of the NEMA method is recommended in the case of images with the smallest possible pixel size. The FWHM of the summed profile and the averaged FWHM of each profile were almost identical. When line profiles were rotated in the images, it was necessary to rotate them to align with an axis.

Based on the physical characteristics of the GATE simulation, further studies using a real camera could be expected to produce results within acceptable errors range (5% overall). The GATE simulation provides reliable virtual experiments. Therefore, it is very useful for developing novel algorithms.

ACKNOWLEDGMENTS

This work is the result of research activities of the Advanced Biometric Research Center (ABRC), which supported by the Korea Science and Engineering Foundation.

REFERENCES

[1] S. Jan, G. Santin, D. Strul, S. Staelens, K. Assie, D. Autret, S. Avner and R. Barbier *et al.*, Phys. Med. Biol. **49**, 4543 (2004).

[2] S. Agostinelli, J. Allison, K. Amako, J. Apostolakis and H. Araujo *et al.*, Nucl. Instr. Meth. A **506**, 250 (2003).

[3] M. Tanaka, S. Uehara, A. Kojima and M. Matsumoto, Phys. Med. Biol. **52**, 4409 (2007).

[4] C. R. Schmidtlein, A. S. Kirov, S. A. Nehmeh, Y. E. Erdi, J. L. Humm, H. I. Amols, L. M. Bidaut, A. Ganin, C. W. Stearns, D. L. McDaniel and K. A. Hamacher, Med Phys. **33**, 198 (2006).

[5] F. Lamare, A. Turzo, Y. Bizais, C. C. Le Rest and D. Visvikis, Phys. Med. Biol. **51**, 943 (2006).

[6] K. Assie, I. Gardin, P. Vera and I. Buvat, Phys. Med. Biol. **50**, 3113 (2005).

[7] D. Lazaro, I. Buvat, G. Loudos, D. Strul, G. Santin, N. Giokaris, D. Donnarieix, L. Maigne, V. Spanoudaki, S. Styliaris, S. Staelens and V. Breton, Phys. Med. Biol. **49**, 271 (2004).

[8] K. Assie, V. Breton, I. Buvat, C. Comtat, S. Jan, M. Krieguer, D. Lazaro, C. Morel, M. Rey, G. Santin, L. Simon, S. Staelens, D. Strul, J.-M. Vieira and R. V. D. Walle, Nucl. Instr. Meth. A **527**, 180 (2004).

[9] S. Staelens, D. Strul, G. Santin, S. Vandenberghe, M. Koole, Y. D'Asseler, I. Lemahieu and R. Van de Walle, Phys Med Biol. **48**, 3021 (2003).

[10] M. Ljungberg, S. E. Strand and M. A. King, *Monte Carlo Calculations in Nuclear Medicine: Applications in Diagnostic Imaging* (IOP, London, 1998).

[11] J. De Beenhouwer, S. Staelens, D. Kruecker, L. Ferrer, Y. D'Asseler, I. Lemahieu and F. R. Rannou, Med Phys. **34**, 1926 (2007).

[12] NEMA, Performance Measurements of Scintillation Cameras, NU 1-2001, NEMA Standards Publication, 2001.

[13] E. W. Weisstein, Full Width at Half Maximum[citated at http://mathworld.wolfram.com/ FullWidthatHalfMaximum.html].

[14] L. P. Ekström and R. B. Firestone, WWW Table of Radioactive Isotopes [citated at http://ie.lbl.gov/toi/].

[15] N. Vinberg and K. Kristensen, European J. Nucl. Med. Mol. **5**, 435 (1980).